Optimal Selection of Phase Encodings in Parallel MR Imaging

Mathews Jacob, Dan Xu, Zhi-Pei Liang

Beckman Institute, University of Illinois at Urbana-Champaign

INTRODUCTION:

Parallel imaging schemes like SENSE [1] and SPACE-RIP [2] accelerate the data acquisition in MRI by using multiple receiver coils. However, in practical applications, it is difficult to obtain speedup factors of the order of the number of coils (critical sampling case). One of the reasons is the redundancy in the measurements due to the inappropriate choice of sampling locations; this leads to the reconstructions being ill-posed for high speed-up factors. Kyriakos et. al. demonstrated that a heuristic choice of the phase encoding locations can give better reconstructions [2]. A more theoretical approach was introduced in [3], where they assumed the signal to be a stationary Gaussian random process and derived the optimal *k*-space lines that result in the minimum mean-squared-error (MMSE) reconstruction.

In this paper, we propose a fast method for selecting the optimal phase encoding locations. In contrast to [3], our algorithm only makes use of the sensitivity profiles and hence is signal independent. We generalize the sequential backward selection (SBS) [4] to derive a fast algorithm. We also show that the reconstructions are robust with respect to estimation errors in the coil sensitivity profiles.

PROPOSED APPROACH:

A. Problem statement

We have a phased array of L coils and we assume an $N \times N$ image. In this paper, we restrict ourselves to the Cartesian scheme as in [3]; we choose M phase encoding lines out of the N uniformly spaced ones (each with N samples along the read-out direction) that gives the minimum mean squared reconstruction error. Our goal is to make M approach its lower bound N/L, while giving well-conditioned reconstructions.

We consider the same imaging equation as in [2]

$$\tilde{S}\vec{\rho} = \tilde{\vec{d}}\,, \tag{1}$$

where the ($N^2 \times 1$) vector $\vec{\rho}$ is the vectorized image, $\tilde{S}$ is obtained by choosing LMN rows of the $LN^2 \times N^2$ matrix S. Similarly $\tilde{\vec{d}}$ is obtained from $\vec{d}$ (vectorization of the measurements) by choosing its corresponding elements. Assuming Gaussian noise and minimum variance solution of Eq. (1) ($\vec{\rho}_{MV} = (\tilde{S}^H \Psi^{-1} \tilde{S})^{-1} \tilde{S}^H \Psi^{-1} \tilde{\vec{d}}$), the sum-of-squared error (SSE) of the reconstructed image is

$$\mathrm{E}\left(\left\|\vec{\rho} - \vec{\rho}_{MV}\right\|^2\right) = \mathrm{trace}\left((\tilde{S}^H \Psi^{-1} \tilde{S})^{-1}\right), \tag{2}$$

where Ψ is the receiver noise matrix [1]. For simplicity, we consider the case where Ψ is identity matrix. The general case can be dealt with by using a Cholesky factorization [5] of matrix Ψ followed by change of variables. Thus, the optimal selection procedure boils down to the selection of the $LMN \times N^2$ sub-matrix $\tilde{S}$ that gives the smallest value of (2).

B. Fast Algorithm

The exhaustive search for the M best phase encoding locations is a combinatorial optimization problem; its complexity is prohibitive for our application. Hence, we generalize the SBS algorithm [4] to seek a slightly sub-optimal, but fast solution. Specifically, we start from the full encoding matrix S and sequentially eliminate blocks of N rows (each block correspond to N samples of one phase encode line). At each step, we eliminate that block which gives the least increment in the cost. Instead of directly calculating Eq. (1), we recursively update its value according to Sherman-Morrison formula [5]. We use a series of speed-up techniques such as storing $(\tilde{S}^H \tilde{S})^{-1} S^H$ and utilizing the separability of 2D FFT. The whole process continues until we are left with M phase encodings.

The algorithm needs $O(N^4)$ multiplies, as compared to $O(N^6)$ multiplies if (2) were used directly. The time taken for optimizing the phase encoding locations for a 128×128 image is about 15 minutes on a 2.66GHz PC.

C. Sensitivity Analysis

In practical applications, the sensitivity profiles are estimated; the estimation errors can lead to degradation of image quality. Denoting $f(S^*)$ as SSE in the reconstruction corresponding to the optimal S^*, we obtain

$$\frac{\left|f(S^* + \Delta S^*) - f(S^*)\right|}{\left|f(S^*)\right|} \le 2\kappa(S^*) \frac{\left\|\Delta S^*\right\|_F}{\left\|S^*\right\|_F}, \tag{3}$$

where $\kappa(S^*)$ is the condition number of S^*. The above formula indicates that the drop off in the image quality is decided by the condition number of $\tilde{S}$; we can effectively reduce it by adding a few more phase encodes as shown in Fig 2.

RESULTS:

Figure 1 shows the simulation results of the proposed algorithm with comparison to reconstruction from sets of lines in [2] using a 128×128 torso image. Four Gaussian-shaped sensitivity profiles are used with different orientations (one of them is shown in Fig. 2.a). It can be easily seen from Fig. 1 that the proposed algorithm outperforms the conventional approaches. See the caption for details.

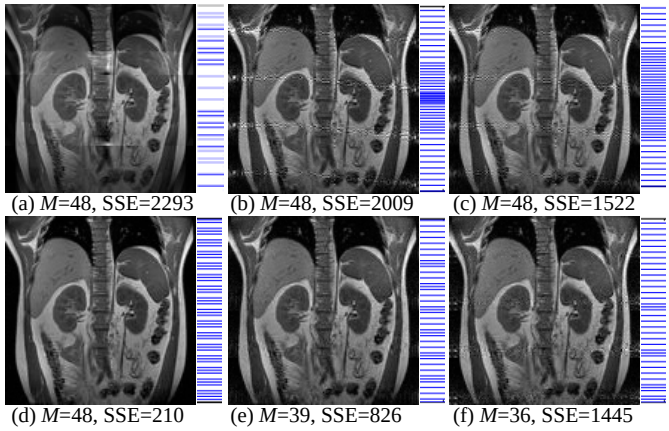

(a) M=48, SSE=2293 (b) M=48, SSE=2009 (c) M=48, SSE=1522

(d) M=48, SSE=210 (e) M=39, SSE=826 (f) M=36, SSE=1445

Figure 1: Simulation results using different phase encoding lines. $N = 128$, $L = 4$. The number of phase encoding lines and the reconstruction SSE are shown below each subfigure. (a) corresponds to SENSE [1] while (b-c) correspond to patterns proposed in SPACE-RIP [2] for a speedup factor of 2.66. Note that the proposed method (d) results in a significantly better reconstruction in terms of reducing both SSE and image artifacts. (e-f) correspond to the reconstructions at higher speed up factors (3.28 and 3.55 respectively). Note that the SSE is lower than (a-c) even with smaller number of lines.

In Figure 2, we show that the proposed algorithm is robust to small perturbations in the coil profiles. By adding a few phase encoding lines, the drop-off of the image quality becomes less sensitive to perturbations of the coil profiles. See the caption for details.

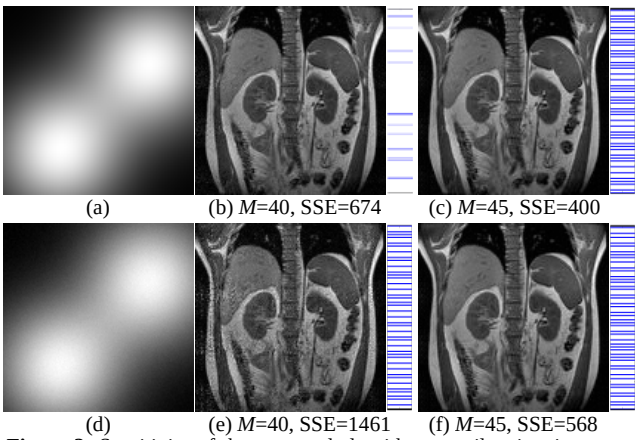

(a) (b) M=40, SSE=674 (c) M=45, SSE=400

(d) (e) M=40, SSE=1461 (f) M=45, SSE=568

Figure 2: Sensitivity of the proposed algorithm to coil estimation errors. We assume that the data is generated by the true profile given in (a) while the estimated profile is its noisy version in (d). (b) and (e) are the reconstructions using 40 lines optimized upon (a) and (d), respectively. As expected, (e) has artifacts due to ill-conditioning and sensitivity map estimation errors as compared to (b). (c) and (f) are reconstructions using 45 lines each optimized upon (a) and (d), respectively. Note that by adding 5 lines, (f) is closer to (c) than (e) to (b). This is well explained by Eq. (3); with 5 more lines, the condition number is smaller that makes the drop-off in image quality less sensitive.

REFERENCES:

[1] K. P. Pruessmann et al., MRM, vol. 42, pp. 952-962, 1999.
[2] W. E. Kyriakos et al., MRM, vol. 44, pp. 301-308, 2000.
[3] N. Aggarwal et al., Proc. ISBI 2004, Washington DC.
[4] S. J. Reeves et al., IEEE Trans. SP, vol. 47, pp. 123-132, 1999.
[5] G. H. Golub et al., Matrix Computations, 3rd Ed., JHU Press, 1996.